

# A NEW METABOLISM MODEL FOR HUMAN SKELETAL MUSCLE

Dayu Lv and Bill Goodwine

Department of Aerospace and Mechanical Engineering, University of Notre Dame, Notre Dame, IN 46556, USA  
dlv@nd.edu, jgoodwin@nd.edu

Keywords: Glucose, Insulin, Skeletal Muscle, Metabolism.

Abstract: The human body metabolic regulatory system is very complex, containing thousands of metabolites involved in biochemical reactions. Glucose metabolism is one of the key procedures maintaining daily energy balance. Mobility of glucose is implemented by glucose transporters with different transporting characteristics locally, which are distributed in cells of brain, liver, pancreas, kidney and skeletal muscle, *etc.* This paper presents a component of a new model that is focused on skeletal muscle which consume energy consistently due to either slight movement or high-energy demanded activities, such as running or swimming. This paper presents a mathematical model where glucose, insulin, glucose-6-phosphate (G6P), *etc.* are introduced and connected by ordinary differential equations.

## 1 INTRODUCTION

This paper presents a new model for the metabolic regulation of glucose in skeletal muscle in humans. It is part of a larger effort to develop a detailed whole-body human metabolic regulation model. Modeling of such systems is useful for several reasons. First, the mathematical structure of an accurate model will provide concise insight into the relevant physiology and also the pathophysiology of disease. Second, it will allow for inexpensive “experimentation” or biosimulation, which if predictive, can serve as a supplement to, and perhaps provide guidance to, *in vivo* and *in vitro* experimentation.

Of course this work is motivated by the epidemic of diabetes, which is a disease characterized by a failure to regulate blood glucose level. Many models have been constructed to describe glucose mobility in humans. What distinguishes this work from others is the scope, or dimension, of the model.

For many years, people have been investigating pathways of carbohydrates metabolism in order to establish mathematical models to reflect biology and control mechanisms. In (Srinivasan et al., 1970), a model composed of glucose, insulin and fatty acids was proposed to explain a two-hour metabolism responding to IV infusions of glucose, insulin, *etc.* Later, another hormone, glucagon, was added to a glucose-insulin system, (Cobelli et al., 1982). A few

years ago, the mass of  $\beta$ -cells was connected to the system of glucose and insulin (Topp et al., 2000). Others were interested at kinetic properties of hormones, particularly insulin. A three-compartment insulin model was introduced in (Sherwin et al., 1974). It was composed of a plasma compartment, a quick compartment equilibrating with plasma and a slower one. Also the pulsative characteristic of insulin was well simulated (Tolić et al., 2000).

Although many models have been proposed, they are mainly restricted to metabolites without reflecting transporters’ activities. In contrast, the model presented in this paper includes details regarding effects of, for example, various glucose transporters (GLUTs) in different organs, as well as *G6P*, which plays a key role in metabolism participating glycogenesis, glycogenolysis and glycolysis.

## 2 MODEL CONSTRUCTION

Skeletal muscle is actively involved in daily life. So the initial focus of our investigation into modeling whole-body glucose metabolism will be skeletal muscle. This model is constituted of two main parts: the interstitial fluid space (*IFS*) and the intracellular space (*ICS*). In the *IFS*, cells are surrounded by a liquid environment for nutrition exchange. *Via* diffusion, glu-

glucose passes through capillaries to the *IFS*, then enter the *ICS* mediated by GLUT4. In the *ICS*, glucose is converted to G6P for storage and utilization. Glycogen can also break down to form G6P.

## 2.1 Intercellular Transport

The mechanism for glucose transport in the *IFS* is illustrated in Figure 1. It is assumed to diffuse through capillaries into the *IFS* and the direction is determined by the difference of glucose concentration between them, given by

$$f_{gs} = K_{01} \times ([G] - [G]_{si}), \quad (1)$$

where  $f_{gs}$  is positive for glucose out of plasma.

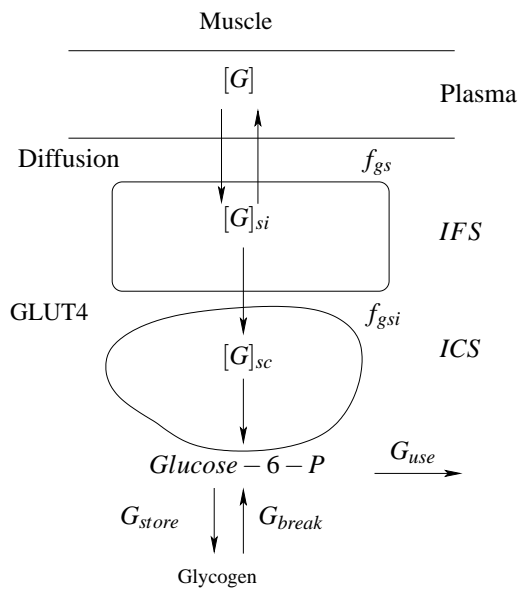


Figure 1: Three compartments of skeletal muscle.

Mediated by GLUT4, glucose is carried into the *ICS* described by Michaelis-Menton kinetics with  $V_{\max} = 1.0$  mmol/kg-muscle/min and  $K_m = 5.7$  mM in the basal state (Perriott et al., 2001). Insulin and exercise may stimulate more GLUT4 activity. The rates of insulin stimulation can be determined from (Sarabia et al., 1992), and exercise from (Fujimoto et al., 2003) and are given by

$$In_V = \frac{1.4331}{1 + e^{-0.2473 \times \lg([In]/(16.7 \times 10^{-10})) - 3.271}} \quad (2)$$

$$Ex_V = \frac{4.4531}{1 + e^{-198.5 \times (\dot{V}_{O_2}/\dot{V}_{O_2 \max}) + 60.95}} + 1, \quad (3)$$

$$V_{\max} = 1.0 \times Mass \times In_V \times Ex_V, \quad (4)$$

where  $[In]$  represents insulin concentration in plasma,

$In_V$  represents the insulin effect on  $V_{\max}$  and  $Ex_V$  represents the exercise effect on  $V_{\max}$ . Consequently, the glucose exchange rate between the *IFS* and the *ICS* is

$$f_{gsi} = -V_{\max} \frac{[G]_{si}}{K_m + [G]_{si}}, \quad (5)$$

where  $[G]_{sc}$  and  $[G]_{si}$  represents the glucose concentration in the *ICS* and the *IFS* respectively,  $f_{gsi}$  represents the rate which is positive for glucose transported out of the *ICS*.

In the model, insulin concentration is only considered in plasma, which is stimulated by increasing glucose concentration determined by dose-response on the secretion of insulin from isolated human islets of Langerhans (Frayn, 2003) and the data are fitted as

$$In_g = \left( \frac{79.21}{1 + e^{-1.934 \times [G] + 10.52}} + 29.84 \right) \times \frac{n \times 0.7}{V_p \times 60}, \quad (6)$$

where  $In_g$  represents the glucose stimulation on insulin secretion (mU/l/min),  $n$  represents the number of Langerhans, approximately one million (Frayn, 2003) assuming 70% of which are  $\beta$ -cells and  $V_p$  represents the plasma volume.

The degradation of insulin ( $In_d$ , mU/l/min), is modeled by a half-life given by

$$In_d = [In] \times e^{-K_{02} \times t}, \quad (7)$$

where  $[In]$  represents insulin concentration in plasma and  $K_{02}$  represents the half-life coefficient (assuming  $K_{02} = 20$ ). Therefore the dynamics of insulin concentration is

$$\frac{d[In]}{dt} = In_d + In_g. \quad (8)$$

## 2.2 Intracellular Space

After glucose uptake, it enters the intracellular metabolic process illustrated in Figure 2. The construction is based on an energy balance where the concentration of ATP remains almost constant (Frayn, 2003). G6P is generated from glucose and glycogen, and utilized through aerobic and anaerobic processes.

### 2.2.1 ATP Conservation

To meet the energy need of *Work* (mol/min), ATP is generated from aerobic and anaerobic glycolysis, the difference between which is the amount of ATP produced. Assuming oxygen is fully utilized by muscle, about 30 mol ATP is generated from 1 mol G6P and

6 mol oxygen (*Aerobic* - mol/min, G6P consumed) while in anaerobic glycolysis (*Anaerobic*, mol/min, G6P consumed), only 2 mol ATP is produced from 1 mol G6P. Also, converting glucose to G6P ( $Rate_1$ , mol/min, G6P produced) and synthesis of G6P to glycogen ( $Syn$  - mol/min, glycogen produced) are consuming energy. The energy of *Work* can be expressed as metabolic rate (Frayn, 2003). While this paper focuses on glucose metabolism, it is important to note that in the Randle-cycle, with competition between glucose and fatty acids, under different intensities of exercises, the proportion of fuels utilization between glucose and FFA will change. For example, under rest or light housework, the proportion of glucose as a fuel is providing about 10% of required energy while during swimming it will increase to about 70%. This is expressed by

$$ATP_{O_2} = \frac{1.429 \times 5}{32} \times \dot{V}_{O_2}, \quad (9)$$

$$Aerobic = \frac{1.429}{32 \times 6} \times \dot{V}_{O_2}, \quad (10)$$

where the oxygen has the density of 1.429 g/l and mole mass of 32 g/mol,  $ATP_{O_2}$  represents the ATP generated by aerobic respiration and *Aerobic* represents the G6P consumed during aerobic respiration. Then *Anaerobic*, the needed rate of G6P for anaerobic glycolysis can be calculated from

$$ATP_{O_2} - Rate_1 + Anaerobic \times 3 - Syn \times 20 = Work, \quad (11)$$

where  $Rate_1$  represents the rate from glucose to G6P and  $Syn$  represents the synthesis rate of glycogen.

### 2.2.2 Glycogen Conservation

Glycogen conservation is simply determined by the synthesis and breakdown rates, given by

$$Syn - Dwn = \Delta(GLY). \quad (12)$$

### 2.2.3 G6P Conservation

Glycogen is a highly branched polymer that can be looked on as a set of multi-G6Ps. In this model, the proportion of glycogen to G6P is assumed to be 1:10 and the change of G6P is given by

$$\Delta G6P = Rate_1 + 10Dwn - 10Syn - Aerobic - Anaerobic. \quad (13)$$

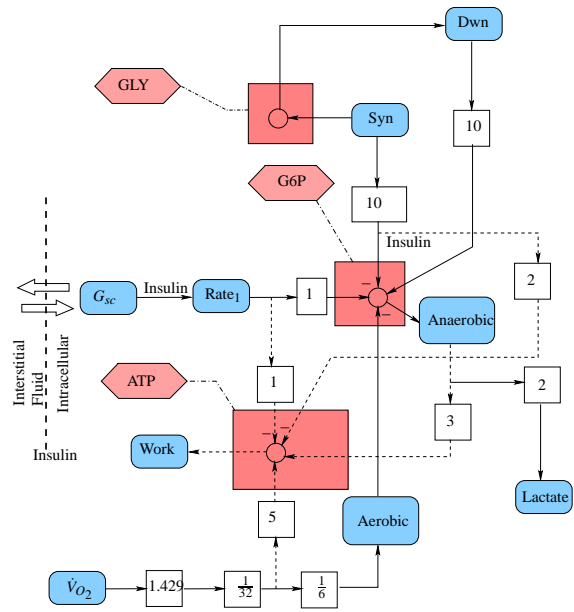


Figure 2: ATP Metabolism in Muscle.

### 2.2.4 Variables

- $Rate_1$  is the hexokinase (*HK*) rate on converting glucose to G6P. Under 456 pM of insulin,  $Rate_1$  was determined as 0.0048 mmol/kg-muscle/min (Rothman et al., 1992). Assuming
  1.  $Rate_1$  is a sigmoidal function of insulin concentration;
  2.  $Rate_1$  is a sigmoidal function of [G6P]; and
  3.  $Rate_1$  is a sigmoidal function of  $[G]_{sc}$ ,

$$R_0 = 1.5 \times Mass, \quad (14)$$

$$In_R = \frac{2}{1 + e^{-(In) + 40.0)/20}}, \quad (15)$$

$$G6P_R = \frac{2}{1 + e^{([G6P] - 0.12 \times Mass / V_{sc})/10}}, \quad (16)$$

$$G_{sc_R} = \frac{2}{1 + e^{-[G]_{sc} + 3.0}}, \quad (17)$$

$$Rate_1 = R_0 \times In_R \times G6P_R \times G_{sc_R}, \quad (18)$$

where  $R_0$  is the basal value,  $Mass$  represents muscle weight,  $In_R$ ,  $G6P_R$  and  $G_{sc_R}$  represents their effects on  $Rate_1$  respectively,  $[In]$ ,  $[G6P]$  and  $[G]_{sc}$  represents concentrations respectively,  $V_{sc}$  represents the volume of the ICS.

- The synthesis rate of glycogen,  $Syn$ , is determined by the concentration of glycogen and G6P, insulin fitted from the data (Kelley and Mandarino, 1990), presented in Table 1 giving

$$GLY_{syn} = \frac{1}{1 + e^{[GLY] - 0.95 \times [GLY]_{max}}}, \quad (19)$$

$$In_{syn} = \frac{2}{1 + e^{-2.2765 \times \lg \frac{[In]}{[In]_0}}} \times \quad (20)$$

$$\frac{2}{1 + e^{0.3517 \times \lg \frac{[G6P]}{[G6P]_0}}}, \quad (21)$$

$$G6P_{syn} = 0.15 \times e^{\lg \frac{[G6P]}{[G6P]_0}}, \quad (22)$$

where  $[GLY]$  and  $[GLY]_{max}$  represents current and maximum glycogen concentration,  $In_{syn}$  and  $G6P_{syn}$  represents their effects on  $Syn$  respectively. Referring to the data,  $[In] = 28.2 \pm 4.2$  pM,  $[G6P] = 0.133 \pm 0.014$  mM, glycogen synthesis rate (mM/hr) was

$$Syn_1 = \begin{cases} 15.8 \pm 1.7, & [GLY] < 35 \text{ mM} \\ 2.9 \pm 0.2, & [GLY] > 35 \text{ mM} \end{cases} \quad (23)$$

(Price et al., 1996). In the model, we assume  $Syn_0 = Syn_1 \times 8$  for reasonable simulation results, and thus

$$Syn = Syn_0 \times In_{syn} \times G6P_{syn} \times GLY_{syn}. \quad (24)$$

Table 1: Insulin(Basal: 9.6 mU/I; Clamp  $77 \pm 3$ mU/I) and G6P (0.1mM; 10mM) effects on  $Syn$ .

| Activity | Basal           | Clamp           |
|----------|-----------------|-----------------|
| 0.1 mM   | $1.59 \pm 0.29$ | $2.82 \pm 0.43$ |
| 10 mM    | $6.14 \pm 0.62$ | $7.21 \pm 0.67$ |

- The breakdown rate of glycogen,  $Dwn$ , is determined by G6P, glycogen and insulin concentrations as follows

$$In_{dwn} = \frac{2}{1 + e^{[In] - 20.0}}, \quad (25)$$

$$G6P_{dwn} = \frac{2}{1 + e^{[G6P] - 1.8}}, \quad (26)$$

$$GLY_{dwn} = \frac{1}{1 + e^{-[GLY] + 0.1 \times [GLY]_{max}}}, \quad (27)$$

where  $[In]$ ,  $[G6P]$ ,  $[GLY]$  and  $[GLY]_{max}$  represents the concentrations of insulin, G6P, glycogen and maximum glycogen. Assuming variables of needed G6P ( $G6P_1$ ) and of test ( $test_1$ ):

$$G6P_1 = Anaerobic + Aerobic + 10Syn(28)$$

$$test_1 = G6P_1 - 0.5 \times \text{current G6P}. \quad (29)$$

If  $test_1$  is near or less than zero, which means current  $G6P$  is enough for consumption, we set the rate (mol/min) as Equation 30 and otherwise as Equation 31,

$$Dwn_0 = 0.02, \quad (30)$$

$$Dwn_0 = test_1 \times 30 \times 10^{-3} / dt, \quad (31)$$

$$Dwn = Dwn_0 \times In_{dwn} \times G6P_{dwn} \times GLY_{dwn}. \quad (32)$$

### 3 SIMULATION RESULTS

Assuming glucose clamp  $[G] = 5$  mM, the simulations assume the following activity plans

- 4 hours rest;
- 1hr rest + 40min light housework + 2hr20min rest;
- 1hr rest + 40min swimming + 2hr20min rest.

and shown in Figures 3 through 7.

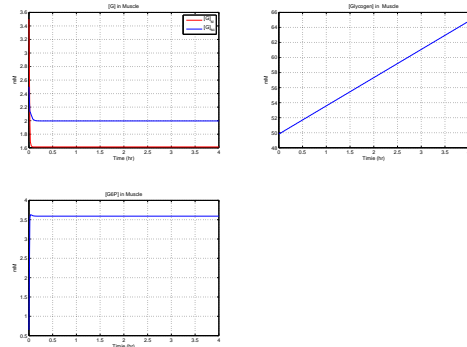


Figure 3: 4hr rest.

For the plan of swimming, we also simulate it with higher glucose levels  $[G] = 7$  mM and  $[G] = 14$  mM, and the results are illustrated in Figures 6 and 7. Note that in Figure 7, intracellular glucose concentration increase rapidly in the last part of simulation, which is due to the saturation of muscle glycogen and  $G6P$ , and it may bring about critical health problems.

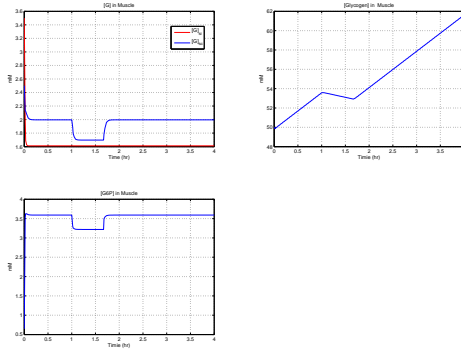


Figure 4: 1hr rest + 40min light housework + 2hr20min rest.

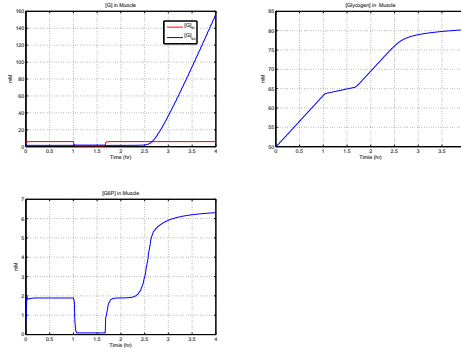


Figure 7:  $[G] = 14$  mM, swimming.

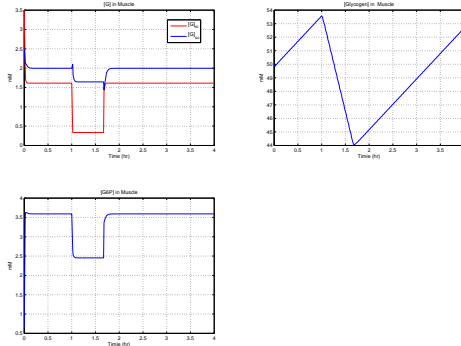


Figure 5: 1hr rest + 40min swimming + 2hr20min rest.

#### 4 CONCLUSIONS AND PERSPECTIVES

In this paper, we have presented a mathematical metabolism model in human muscle. It is based on

the kinetics of glucose transporters, GLUT4 and also considers the key role of *G6P*, whose regulation will determine the flow between storage and utilization. It works well in simulations. Under different activities, it reflects the interrelationships among glucose, insulin, *G6P* and glycogen.

The model has some limitations which we are currently addressing. First, the role of the glucose transporter GLUT1, with different kinetics is not yet considered. This transporter clearly plays a role in the basal state. Second, insulin concentration is considered only in plasma for simplification. And third, experiment data are still needed for a few of the equations. We indicated throughout the paper where a numerical value had to be assumed. Subsequent work will include a series of numerical experiments to better define the value, or range of values, that are feasible for such parameters.

In future work, the dynamics of insulin will be investigated and improved. Its resistance due to lasting high glucose level may be considered. Also, during exercises, increased level of lactate may be connected to other organs, such as liver. The overall goal, as mentioned previously, is a whole-body model expressed at a level of detail and fidelity similar to that for the muscle presented in this paper.

#### ACKNOWLEDGEMENTS

Partial support from the Center for Applied Mathematics of University of Notre Dame and the Notre Dame Faculty Research Program are gratefully acknowledged.

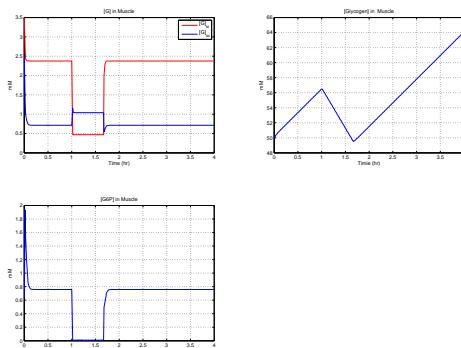


Figure 6:  $[G] = 7$  mM, swimming.

## REFERENCES

- Cobelli, C. et al. (1982). An integrated mathematical model of the dynamics of blood glucose and its hormonal control. *Mathematical Biosciences*, 58:27–60.
- Frayn, K. N. (2003). *Metabolic Regulation: A Human Perspective*. Blackwell Science Ltd, Oxford, 2nd edition.
- Fujimoto, T. et al. (2003). Skeletal muscle glucose uptake response to exercise in trained and untrained men. *Med. Sci. Sports Exerc.*, 35:777–783.
- Kelley, D. E. and Mandarino, L. J. (1990). Hyperglycemia normalizes insulin-stimulated skeletal muscle glucose oxidation and storage in noninsulin-dependent diabetes mellitus. *J. Clin. Invest.*, 86:1999–2007.
- Perriott, L. M. et al. (2001). Glucose uptake and metabolism by cultured human skeletal muscle cells: rate-limiting steps. *Am. J. Physiol. Endocrinol Metab.*, 281:72–80.
- Price, T. B. et al. (1996). Nmr studies of muscle glycogen synthesis in insulin-resistant offspring of parents with non-insulin-dependent diabetes mellitus immediately after glycogen-depleting exercise. *Proc. Natl. Acad. Sci. USA*, 93:5329–5334.
- Rothman, D. L. et al. (1992). <sup>31</sup>p nuclear magnetic resonance measurements of muscle glucose-6-phosphate. *J. Clin. Invest.*, 89:1069–1075.
- Sarabia, V. et al. (1992). Glucose transport in human skeletal muscle cells in culture. *J. Clin. Invest.*, 90:1386–1395.
- Sherwin, R. S. et al. (1974). A model of the kinetics of insulin in man. *J. Clin. Invest.*, 53:1481–1492.
- Srinivasan, R. et al. (1970). A mathematical model for the control mechanism of free fatty acid-glucose metabolism in normal humans. *Computers and Biomedical Research*, 3:146–166.
- Tolić, I. M. et al. (2000). Modeling the insulin-glucose feedback system: the significance of pulsatile insulin secretion. *J. Theor. Biol.*, 207:361–375.
- Topp, B. et al. (2000). A model of  $\beta$ -cell mass, insulin, and glucose kinetics: pathways to diabetes. *J. Theor. Biol.*, 206:605–619.

|                               |          |  |
|-------------------------------|----------|--|
| $G/[G]$                       | mmol/mM  | Glucose amount/concentration in plasma.              |
| $G_{si}/[G]_{si}$             | mmol/mM  | Glucose amount/concentration in interstitial space.  |
| $G_{sc}/[G]_{sc}$             | mmol/mM  | Glucose amount/concentration in intracellular space. |
| $G6P/[G6P]$                   | mmol/mM  | G6P amount/concentration                             |
| $[In]$                        | mU/l     | Insulin concentration.                               |
| $\dot{V}O_2/\dot{V}O_{2\max}$ | l/min    | Oxygen consumption rate/Maximum.                     |
| $Mass$                        | kg       | Skeletal muscle weight,                              |
| $n$                           | N/A      | Number of Langerhans                                 |
| $V_{si}/V_{sc}$               | 1        | Volume of interstitial space /intracellular space.   |
| $V_b/V_p$                     | 1        | Blood/Plasma Volume.                                 |
| $GLY/GLY_{\max}$              | mM       | Glycogen concentration /Maximum concentration.       |
| $V_{\max}$                    | mmol/min | Maximum reaction rate.                               |
| $K_m$                         | mM       | Michaelis constant.                                  |
| $K_{01}$                      | l/min    | Diffusion coefficient.                               |
| $K_{02}$                      | N/A      | Insulin half-life coefficient.                       |
| <i>Aerobic</i>                | mol/min  | aerobic glycolysis rate.                             |
| <i>Anaerobic</i>              | mol/min  | anaerobic glycolysis rate.                           |
| <i>Syn</i>                    | mol/min  | Glycogen synthesis rate.                             |
| <i>Dwn</i>                    | mol/min  | Glycogen breakdown rate.                             |

|                    |   |
|--------------------|---|
| $[G]$              | 5   |
| $[G]_{si}$         | 3.5   |
| $[G]_{sc}$         | 2.5   |
| $G6P$              | $0.12 \times Mass$  |
| <i>Body weight</i> | 70  |
| <i>Mass</i>        | 45% of <i>Body weight</i>   |
| $n$                | $10^6$  |
| $[In]$             | 10  |
| $\dot{V}O_2$       | Percentage of $\dot{V}O_{2\max}$ :<br>rest - 10%<br>light housework - 25%<br>swimming - 75% |
| $V_{si}$           | 10% of <i>Mass</i>  |
| $V_{sc}$           | $0.1852 \times Mass$  |
| $V_b$              | 5   |
| $V_p$              | 55% of $V_b$  |
| $GLY_{\max}$       | 1% of <i>Mass</i>   |
| $K_m$              | 5.7   |
| $K_{01}$           | 2   |
| $K_{02}$           | 20  |

## APPENDIX

The variables, parameters and initial values are shown in this appendix.